

# A Simple Method To Synthesize Nanowires

Yingjiu Zhang, Nanlin Wang, Shangpeng Gao, Rongrui He, Shu Miao, Jun Liu, Jing Zhu,\* and X. Zhang

Electron Microscopy Laboratory, School of Materials Science and Engineering, Tsinghua University, Beijing 100084 People's Republic of China

Received February 15, 2002. Revised Manuscript Received May 30, 2002

By a simple method, that is, by heating raw materials in a flowing gas at ambient pressure,  $\text{Si}_3\text{N}_4$ ,  $\text{Ga}_2\text{O}_3$ , and  $\text{ZnO}$  nanowires,  $\text{SiC}$  nanocables, and  $\text{SiO}_2$  amorphous nanowires are synthesized without metal catalysts. The diameters of these one-dimensional nanoscale materials are greatly affected by synthesis temperatures. At suitable synthesis temperatures, their diameters are  $<100$  nm. The growth mechanisms of these nanowires are discussed preliminarily.

## Introduction

One-dimensional (1D) structures with nanometer diameters, such as nanotubes and nanowires, have great potential for testing and understanding fundamental concepts about the effects of dimensionality and size on, for example, mechanical, optical, and electrical properties. Over the past several years, great efforts have been placed on the bulk synthesis of one-dimensional nanoscale materials, and various synthesis methods, such as chemical vapor deposition (CVD),<sup>1</sup> arc discharge,<sup>2</sup> laser ablation,<sup>3</sup> template-assisted growth,<sup>4</sup> solution,<sup>5</sup> and physical evaporation (PE)<sup>6</sup> have been exploited.

Here, we describe a simple method to synthesize a series of nanowires. By heating of raw materials in a flowing gas at ambient pressure,  $\text{Si}_3\text{N}_4$ ,  $\text{Ga}_2\text{O}_3$ , and  $\text{ZnO}$  nanowires,  $\text{SiC}$  nanocables, and  $\text{SiO}_2$  amorphous nanowires have been synthesized. Because no metal catalysts are needed, the nanowires prepared here may have high purity in compositions. Although the above nanowires have been fabricated by now,<sup>7–11</sup> this method has the

advantages of simplicity, low cost, and fewer number of necessary apparatuses. Additionally, the simple method may be extended to fabricate many other one-dimensional nanoscale materials as described below.

## Experimental Section

Raw materials (Table 1) in an  $\text{Al}_2\text{O}_3$  boat were put in the middle of an  $\text{Al}_2\text{O}_3$  tube (1000 mm in length and 35 mm in inner diameter), which was placed in a horizontal furnace (Figure 1a). An inert gas stream at a flow rate of 100–500 sccm (standard cubic centimeter per minute) was introduced into the  $\text{Al}_2\text{O}_3$  tube, when the furnace was started to be heated and was turned out when the temperature of the furnace was cooled to ambient temperature. The materials were heated at desired synthesis temperatures for 1 h, and when the desired temperatures were maintained, the temperature distributions along the  $\text{Al}_2\text{O}_3$  tube were measured, and one of the temperature profiles (when  $\text{SiC}$  nanocables were fabricated) is shown in Figure 1b. In all the experiments, no metal catalysts were introduced. After reaction, the product of  $\text{SiC}$  nanowires

\* To whom correspondence should be addressed. Phone: 86-10-62794026. Fax: 86-10-62772507. E-mail: jzhu@mails.tsinghua.edu.cn.

(1) (a) Wagner, R. S.; Ellis, W. C. *Appl. Phys. Lett.* **1964**, *4*, 89. (b) Westwater, J.; Gosain, D. P.; Tomiya, S.; Usui, S.; Ruda, H. *J. Vac. Sci. Technol.* **1997**, *B15*, 554. (c) Amelinckx, S.; Zhang, X. B.; Bernaerts, D.; Bernaerts, D.; Zhang, X. F.; Ivanov, V.; Nagy, J. B. *Science* **1994**, *265*, 635.

(2) (a) Iijima, S. *Nature* **1991**, *354*, 56. (b) Ebbesen, T. W.; Ajayan, P. M. *Nature* **1992**, *358*, 220. (c) Seeger, T.; Kohler-Redlich, P.; Rühle, M. *Adv. Mater.* **2000**, *12*, 279.

(3) (a) Thess, A.; Lee, R.; Nikolaev, P.; Dai, H.; Petit, P.; Robert, J.; Xu, C.; Lee, Y. H.; Kim, S. G.; Rinzler, A. G.; Colbert, D. T.; Scuseria, G. E.; Tomanek, D.; Fischer, J. E.; Smalley, R. E. *Science* **1996**, *273*, 483. (b) Morales, A. M.; Lieber, C. M. *Science* **1998**, *279*, 208. (c) Yu, D. P.; Lee, C. S.; Bello, I.; Sun, X. S.; Tang, Y. H.; Zhou, G. W.; Bai, Z. G.; Zhang, Z.; Feng, S. Q. *Solid State Commun.* **1998**, *105*, 403. (d) Yudasaka, M.; Komatsu, T.; Ichihashi, T.; Iijima, S. *Chem. Phys. Lett.* **1997**, *278*, 102.

(4) (a) Dai, H. J.; Wong, E. W.; Lu, Y. Z.; Fan, S. S.; Lieber, C. M. *Nature* **1995**, *375*, 769. (b) Han, W. Q.; Fan, S. S.; Li, Q. Q.; Liang, W. J.; Gu, B. L.; Yu, D. P. *Chem. Phys. Lett.* **1997**, *265*, 374. (c) Han, W. Q.; Bando, Y.; Kurashima, K.; Sato, T. *Appl. Phys. Lett.* **1998**, *73*, 3085. (d) Han, W. Q.; Philipp, K. R.; Ernst, F.; Rühle, M. *Chem. Mater.* **1999**, *11*, 3620. (e) Zhang, Y. J.; Zhu, J.; Zhang, Q.; Yan, Y. J.; Wang, N. L.; Zhang, X. *Chem. Phys. Lett.* **2000**, *317*, 504. (f) Zhang, Y. J.; Liu, J.; He, R. R.; Zhang, Q.; Zhang, X.; Zhu, J. *Chem. Mater.* **2001**, *13*, 3899. (g) Han, W. Q.; Fan, S. S.; Li, Q. Q.; Gu, B. L. *Appl. Phys. Lett.* **1997**, *71*, 2271.

(5) Holmes, J. D.; Johnston, K. P.; Christopher, Doty R.; Korgel, B. A. *Science* **2000**, *287*, 1471.

(6) (a) Yu, D. P.; Bai, Z. G.; Ding, Y.; Hang, Q. L.; Zhang, H. Z.; Wang, J. J.; Zou, Y. H.; Qian, W.; Xiong, G. C.; Zhou, H. T.; Feng, S. Q. *Appl. Phys. Lett.* **1998**, *72*, 3458. (b) Zhang, H. Z.; Kong, Y. C.; Wang, Y. Z.; Du, X.; Bai, Z. G.; Wang, J. J.; Yu, D. P.; Ding, Y.; Hang, Q. L.; Feng, S. Q. *Solid State Commun.* **1999**, *109*, 677. (c) Zhang, Y. F.; Tang, Y. H.; Lam C.; Wang, N.; Lee, C. S.; Bello, I.; Lee, S. T. *J. Cryst. Growth* **2000**, *212*, 115. (d) Wang, N.; Zhang, Y. F.; Tang, Y. H.; Lee, C. S.; Lee, S. T. *Appl. Phys. Lett.* **1998**, *73*, 3902. (e) Tang, Y. H.; Zhang, Y. F.; Peng, H. Y.; Wang, N.; Lee, C. S.; Lee, S. T. *Chem. Phys. Lett.* **1999**, *314*, 16. (f) Gole, J. L.; Stout, J. D.; Rauch, W. L.; Wang, Z. L. *Appl. Phys. Lett.* **2000**, *76*, 2346.

(7) (a) Gopalakrishnan, P. S.; Lakshminarasimham, P. S. *J. Mater. Sci. Lett.* **1993**, *12*, 1422. (b) Inomata, Y.; Yamane, T. *J. Cryst. Growth* **1974**, *21*, 317.

(8) (a) Milewski, J. V.; Gac, F. D.; Petrovic, J. J.; Skaggs, S. R. *J. Mater. Sci.* **1985**, *20*, 1160. (b) Zhou, X. T.; Lai, H. L.; Peng, H. Y.; Shang, N. G.; Wang, N.; Bello, I.; Lee, C. S.; Lee, S. T. *Chem. Phys. Lett.* **2000**, *318*, 58. (c) Tang, C. C.; Fan, S. S.; Dang, H. Y.; Zhao, J. H.; Zhang, C.; Li, P.; Gu, Q. *J. Cryst. Growth* **2000**, *210*, 595. (d) Zhang, Y. J.; Wang, N. L.; He, R. R.; Chen, X. H.; Zhu, J. *J. Cryst. Growth* **2001**, *226*, 185.

(9) (a) Wu, X. C.; Song, W. H.; Song, W. D.; Huang, W. D.; Pu, M. H.; Zhao, B.; Sun, Y. P.; Du, J. *J. Chem. Phys. Lett.* **2000**, *328*, 5. (b) Choi, Y. C.; Kim, W. S.; Park, Y. S.; Lee, S. M.; Bae, D. J.; Lee, Y. H.; Park, G.-S.; Choi, W. B.; Lee, N. S.; Kim, J. M. *Adv. Mater.* **2000**, *12*, 746.

(10) (a) Pan, Z. W.; Dai, Z. R.; Wang, Z. L. *Science* **2001**, *291*, 1947. (b) Kong, Y. C.; Yu, D. P.; Zhang, B.; Feng, W.; Feng, S. Q. *Appl. Phys. Lett.* **2001**, *78*, 407. (c) Huang, M. H.; Wu, Y. Y.; Feick, H. N.; Tran, N.; Weber, E.; Yang, P. D. *Adv. Mater.* **2001**, *13*, 113.

(11) Yu, D. P.; Hang, O. L.; Ding, Y.; Zhang, H. Z.; Bai, Z. G.; Wang, J. J.; Zou, Y. H.; Qian, W.; Xiong, G. C.; Feng, S. Q. *Appl. Phys. Lett.* **1998**, *73*, 3076.

**Table 1. Summary of the Products Obtained at Optimum Synthesis Parameters**

product	raw materials	synthesis temp (°C)	carrier gas	diameter (nm)	axis
Si <sub>3</sub> N <sub>4</sub> and SiO <sub>2</sub>	Si or (Si/SiO <sub>2</sub> )	1200–1400	N <sub>2</sub>	for Si <sub>3</sub> N <sub>4</sub> , most are in the range of 15–35 nm. for SiO <sub>2</sub> , <300 nm; most <50 nm.	⊥{0001}
SiO <sub>2</sub>	Si or (Si/SiO <sub>2</sub> )	1100–1300	Ar	most <50 nm	
SiC	SiO <sub>2</sub> , nanoscale C particles	1550	Ar	most <50 nm	⊥{200}
Ga <sub>2</sub> O <sub>3</sub>	Ga	650	N <sub>2</sub> (Ar)	most <50 nm	//(001)
ZnO	Zn	650	N <sub>2</sub> (Ar)	most <50 nm	//(0001)
In	In	1350–1400	Ar	30–40 nm	//(001)

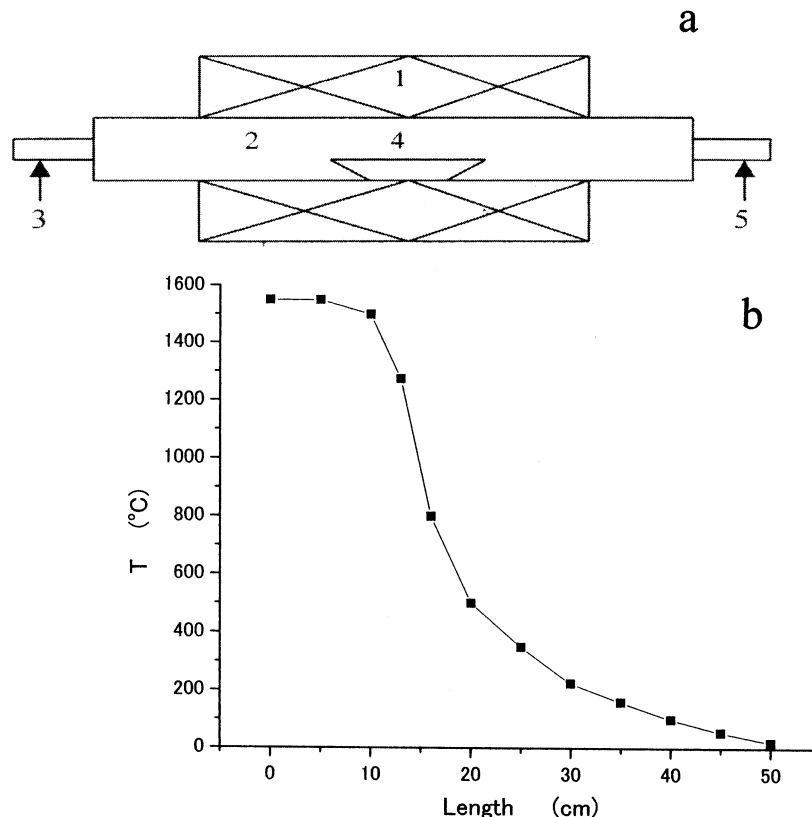


**Figure 1.** Synthesis system and temperature distribution: (a) Synthesis system scheme of the simple method (1) furnace, (2) Al<sub>2</sub>O<sub>3</sub> tube, (3) gas inlet, (4) Al<sub>2</sub>O<sub>3</sub> boat containing raw materials, (5) gas outlet. (b) Temperature profile along the Al<sub>2</sub>O<sub>3</sub> tube, the length indicates the distance between the given position and the center of the Al<sub>2</sub>O<sub>3</sub> tube along its axis.

(nanocables) was deposited as a gray film on the downstream end of the Al<sub>2</sub>O<sub>3</sub> tube, while the products of other nanowires were white flocky films covering the raw materials. The morphologies and atomic structures of the products were characterized by using a scanning electron microscope (SEM, JEM-6301F) and a field-emission gun transmission electron microscope (TEM, JEM-2010F). The TEM was equipped with an energy-dispersive spectrometer (EDS) and an electron energy loss spectrometer (EELS).

### Results and Discussion

Scanning electron microscopy (SEM) photos (Figure 2a–c) show that the products obtained at proper synthesis temperatures are nanowires with a high aspect ratio (length/diameter). Their lengths range from several micrometers to tens of micrometers while their diameters are <100 nm. No droplets are found for any nanowires. The ZnO and Ga<sub>2</sub>O<sub>3</sub> nanowires grow from the corresponding raw materials and are seen as brushwood. However, at higher synthesis temperatures, the nanowires coarsen and the diameters of ZnO, Ga<sub>2</sub>O<sub>3</sub>, and Si<sub>3</sub>N<sub>4</sub> nanowires are larger than 100 nm or even larger than 500 nm (Figure 2d). Moreover, although there is a small droplet on one end of some nanowires synthesized at these higher temperatures, the composi-

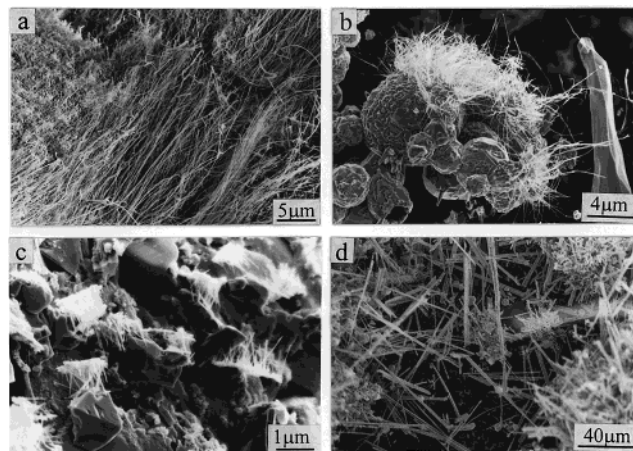


**Figure 2.** Scanning electron microscopy (SEM) images: (a) Si<sub>3</sub>N<sub>4</sub> nanowires, (b) ZnO nanowires, (c) Ga<sub>2</sub>O<sub>3</sub> nanowires, and (d) ZnO nanowires synthesized at higher temperature.

tions of the droplets are the same as those of the corresponding nanowires.

Transmission electron microscopy (TEM) images and electron energy loss spectrum (EELS) provide more detailed information about these nanowires. The image

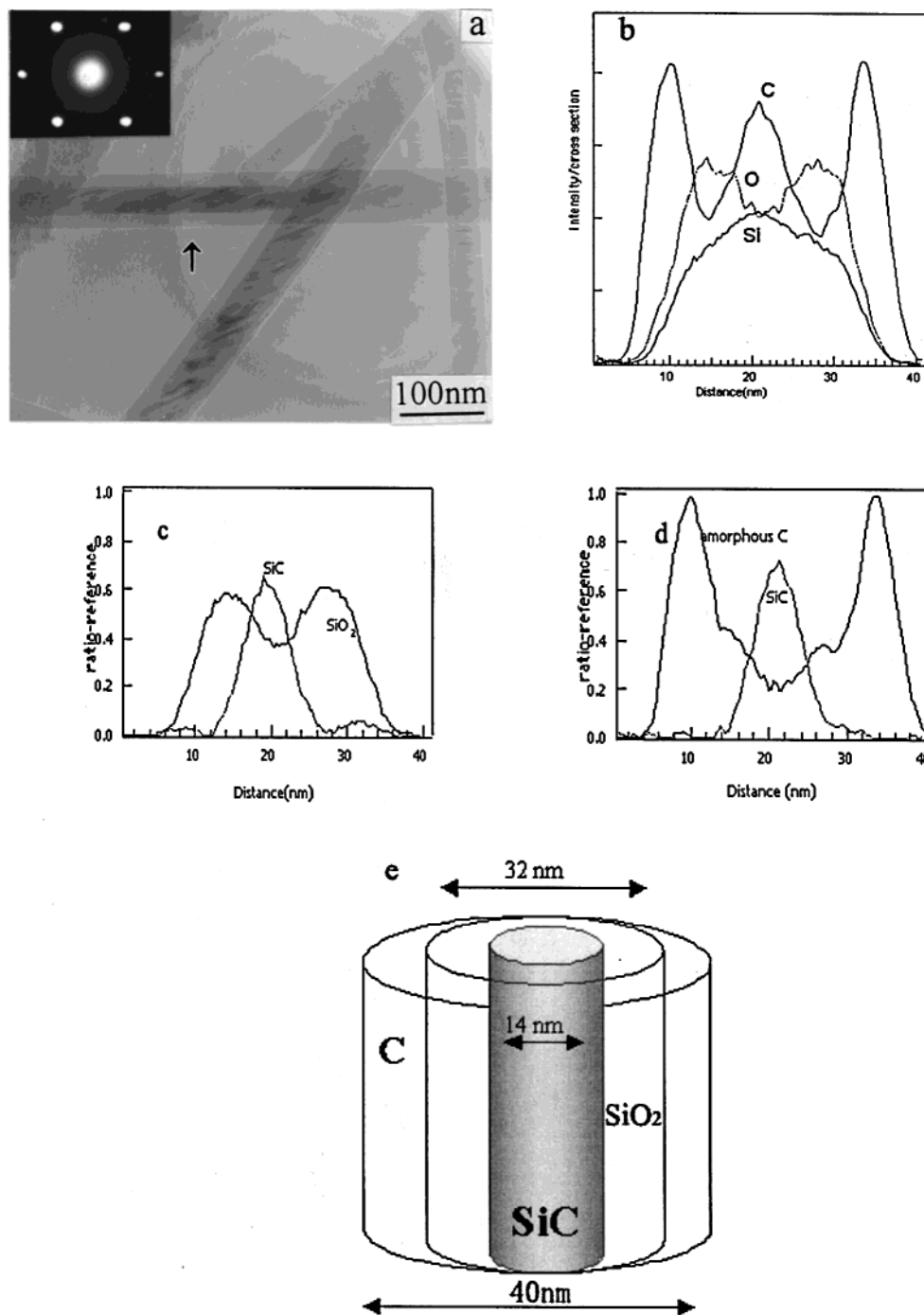


**Figure 3.** EELS and structure of the SiC nanowire: (a) the core of the SiC nanowire (marked by the arrow) is a  $\beta$ -SiC phase with one of the  $\{200\}$  planes perpendicular to its axis; (b) the profiles of C, O, and Si along the direction perpendicular to a SiC nanowire's axis; (c) the distribution of  $\beta$ -SiC and amorphous  $\text{SiO}_2$ ; (d) the distribution of  $\beta$ -SiC and amorphous C; (e) a scheme of the SiC nanowire (nanocable). The core is a  $\beta$ -SiC crystalline phase; the interlayer and the sheath are amorphous  $\text{SiO}_2$  and carbon, respectively.

in Figure 3a shows that the SiC nanowire has a crystalline core with a surrounding amorphous layer. The selected area electronic diffraction (SAED) pattern (insert in Figure 3a) indicates that the crystalline core is  $\beta$ -phase SiC, with one of  $\{200\}$  crystal planes perpendicular to the axis of the nanowire. Elemental profiles across a SiC nanowire with about 40 nm in diameter (not the nanowire in Figure 3a) are obtained by scanning a finely focused electron probe and recording the EELS spectra, and the profiles represent the distribution of atomic concentrations. There are one, two, and three peaks in the profiles of Si, O, and C,

respectively (Figure 3b), which indicates that Si is mainly in the core and interlayer of the nanowire, O is mainly in the interlayer of the nanowire, and C is in the center core and the outer layer of the nanowire. After having been compared with the standard EELS spectra of amorphous C, amorphous  $\text{SiO}_2$ , and  $\beta$ -phase SiC,<sup>12</sup> the distributions of  $\beta$ -SiC, amorphous C, and amorphous  $\text{SiO}_2$  across the nanowire are shown in Figure 3c,d. Thus, the structure of the nanowire can be illustrated as in Figure 3e. The SiC nanowire is a multiphase nanocable and its crystalline core is  $\beta$ -SiC whereas there are two amorphous layers, a  $\text{SiO}_2$  inter-

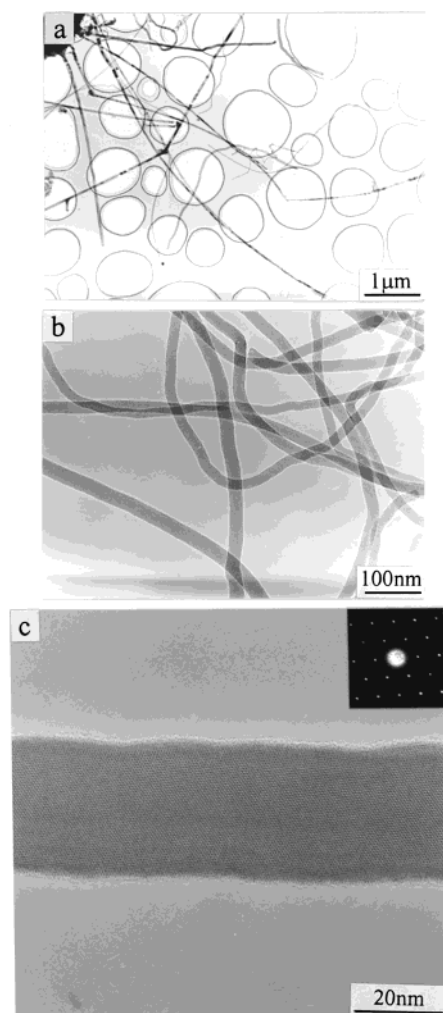


**Figure 4.** TEM images of the  $\text{Si}_3\text{N}_4$  and  $\text{SiO}_2$  nanowire: (a) When  $\text{N}_2$  is used,  $\text{Si}_3\text{N}_4$  nanowires and  $\text{SiO}_2$  amorphous nanowires are fabricated; (b) when Ar is used, only  $\text{SiO}_2$  amorphous nanowires are fabricated; (c) HREM image of a  $\text{Si}_3\text{N}_4$  nanowire; its axis is perpendicular to one of the  $\{0001\}$  planes.

layer and C sheath, surrounding its core. It should be noted that the amorphous C sheath does not result from the deposition of carbon in TEM because there is always an amorphous carbon layer surrounding the SiC nanowire even if we observe the nanowires just for a few seconds. The amorphous C sheath in Si-SiO<sub>2</sub>-C nanowire has been observed by Lee's research group.<sup>13</sup>

If Si or a Si/SiO<sub>2</sub> mixture is heated, it is found that nanowires can be fabricated in bulk and the types of the nanowires change with the different reactant gases. If  $\text{N}_2$  is introduced, crystalline  $\text{Si}_3\text{N}_4$  nanowires with <100 nm (most in 15–35 nm) in diameter (Figure 4a) and amorphous  $\text{SiO}_2$  nanowires with <300 nm (most <50 nm) are synthesized whereas only thinner amorphous  $\text{SiO}_2$  nanowires (most <50 nm) are fabricated if Ar is used (Figure 4b). The high-resolution electron microscopy (HREM) image in Figure 4c shows that the  $\text{Si}_3\text{N}_4$  nanowire is a perfect single crystal with an amorphous layer. The axes of most  $\text{Si}_3\text{N}_4$  nanowires are about perpendicular to one of the  $\{0001\}$  planes as

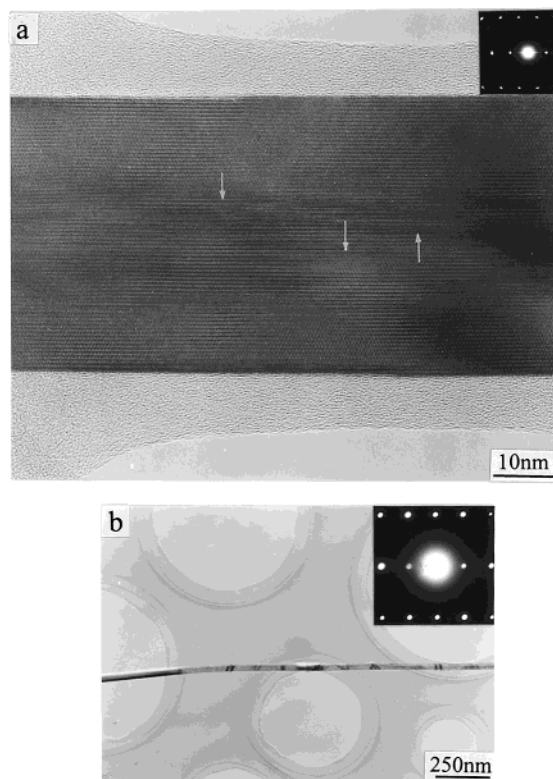


**Figure 5.** TEM images and SAED of  $\text{Ga}_2\text{O}_3$  and ZnO: (a) HREM image of  $\text{Ga}_2\text{O}_3$  nanowire; its axis is parallel to (001) plane and there are some faults marked by the arrows in the nanowire; (b) ZnO nanowire; its growth direction is  $[0001]$ .

shown in Figure 4c and the nanowires are hexagonal structure  $\alpha$  phase  $\text{Si}_3\text{N}_4$ , with crystal lattices of  $a = 0.78$  nm and  $c = 0.56$  nm.

The TEM images of  $\text{Ga}_2\text{O}_3$  and ZnO nanowires are shown in Figure 5. A HREM photo of  $\text{Ga}_2\text{O}_3$  nanowire with its axis parallel to the (001) crystal plane is shown in Figure 5a. It has a monoclinic structure with crystal lattices of  $a = 1.23$  nm,  $b = 0.30$  nm,  $c = 0.58$  nm, and  $\beta = 104^\circ$ . There are some faults marked by the arrows in this nanowire. The ZnO nanowire, on the other hand, is a wurtzite structure and the lattice parameters are  $a = 0.33$  nm and  $c = 0.52$  nm. Its growth direction is  $[0001]$ , consistent with that of the ZnO nanobelt prepared by Wang's research group.<sup>10a</sup>

The synthesis parameters and the properties of the products are listed in Table 1. Moreover, our studies demonstrate that, besides the nanowires mentioned above, other nanowires, such as  $\text{Al}_2\text{O}_3$  and Si nanowires, can be synthesized by this simple synthesis method. Specially, In metal nanowires (unpublished paper) have also been fabricated by this method and the synthesis parameters of this kind of nanowires are also listed in Table 1. There is little work to synthesize metal nanowire (nanobelt) by this method or other CVD and PVD methods.<sup>14</sup> It means that the method introduced here may be extended to fabricating many other kinds of nanowires. However, when  $\text{NH}_3$  or P vapor are introduced and Ga is heated, GaN or GaP nanowires are not obtained. In these cases, although nanowires are also fabricated, it is found that these nanowires are  $\text{Ga}_2\text{O}_3$  nanowires with a small amount of N or P doped. In the

(12) Ahn, C. C.; Krivanek, O. L.; Burgner, R. P.; Disko, M. M.; Swann, P. R.; EELS Atlas, Ajoint project of the ASU HREM facility and GATAN.

(13) Shi, W.-S.; Peng, H.-Y.; Xu L.; Wang, N.; Tang, Y.-H.; Lee, S.-T. *Adv. Mater.* **2000**, *12*, 1927.

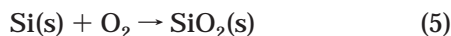
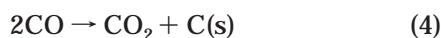
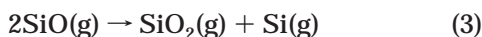
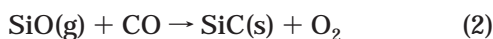
(14) Wang, Y. W.; Zhang, L. D.; Meng, G. W.; Liang, C. H.; Wang, G. Z.; Sun, S. H. *Chem. Commun.* **2001**, *24*, 2632.

present work, no vacuum system is used; therefore, there is always a little residual O<sub>2</sub> in the reaction chamber. Ga reacts easily with O and thus no GaN or GaP but Ga<sub>2</sub>O<sub>3</sub> nanowires are fabricated. As N or P has been doped in the Ga<sub>2</sub>O<sub>3</sub> nanowires, these kinds of Ga<sub>2</sub>O<sub>3</sub> nanowires may have some special properties and need to be further investigated.

In the present work, as mentioned above, no metal catalyst is used and no metal droplet is found when the wires are synthesized at a proper synthesis temperature. At higher synthesis temperature, although there are droplets at the ends of some of the thick wires, the compositions of the droplets are the same as those of the thick wires. Thus, the vapor–solid (VS) growth mechanism is more possible than the vapor–liquid–solid (VLS) one.<sup>15</sup> However, as mentioned above, some kinds of nanowires (In and SiC) are deposited on the downstream end of the Al<sub>2</sub>O<sub>3</sub> tube, whereas other kinds of nanowires are grown on the top surfaces of the reactants (or the surfaces of the boat containing the reactants). It indicates that there is more than one type of growth mechanism in the present work. In the former condition, the reactant vapors are carried by the inert gas stream to the downstream end where the temperature is lower than that in the center of the furnace. Because of the lower temperature (the temperature gradient), the vapors will deposit on the inner surface of the Al<sub>2</sub>O<sub>3</sub> tube. The growth mechanism may be similar to that of the vapor transportation method<sup>15,16</sup> or physical evaporation method.<sup>6b,f,10a,17</sup> During the growth of the nanowires, both the physical process and chemical process are all possible and the unidirectional motion of the reactants atom cloud driven by the carrier gas may play a role in the preferential 1D growth of the nanowires.<sup>14</sup> When In nanowires are fabricated, only the physical process exists. When SiC/SiO<sub>2</sub>/C nanowires are formed, several chemical reactions take place. At high temperature, C particles react with SiO<sub>2</sub> particles at the center of the furnace according to the following reaction:<sup>7a</sup>



The SiO and CO gases are carried by Ar flow to the region of lower temperature and the following reactions will occur there:<sup>4g,7a,8c</sup>



SiC deposits and grows as the crystalline core and SiO<sub>2</sub> and C deposit on the SiC core, and thus the nanowires of the SiC crystalline core, SiO<sub>2</sub> interlayer, and C outer layer are formed.

On the other hand, the growth mechanism of the nanowires grown on the surfaces of the reactants may be through the VS or VLS processes. As no metal

catalysts are used and there are no droplets with metal catalysts on the ends of the nanowires, it is likely that these nanowires follow a growth mechanism similar to the VS one. However, in the growth of ZnO and Ga<sub>2</sub>O<sub>3</sub> nanowires, Zn and Ga, respectively, might act as catalysts (self-catalysts function), even though they will be finally oxidized into ZnO and Ga<sub>2</sub>O<sub>3</sub>. When the Si<sub>3</sub>N<sub>4</sub> nanowires are fabricated, because of the irreversible O<sub>2</sub> in the reaction system, SiO will be generated and an oxide-assisted growth mechanism<sup>6d</sup> may play a role in the growth of the nanowires. In the growth of these nanowires, the relatively lower supersaturation is probably critical for whisker growth, which should be lower than that required for euhedral crystal growth; otherwise, two- or three-dimensional growth will occur.<sup>18</sup> The phenomenon that low supersaturation benefits the growth of the whiskers (nanowires) has been proven by many of works.<sup>19</sup> In the present work, no ZnO nanowires are obtained by heating Zn in air. One reason may be a high supersaturation of ZnO when Zn reacts with excessive oxygen, which induces the formation of the stable ZnO particles. It should be noted that the low supersaturation is a relative concept here; the supersaturation should not be too low. In the Yumoto et al.' work<sup>20</sup> of heating Zn bars to fabricate Zn crystal, no one-dimensional Zn crystals can be fabricated owing to the fast production of Zn vapor (high Zn supersaturation). On the other hand, by the heating of ZnS and C powder, Zn nanobelts are fabricated. In the growth of Zn nanobelts, the product rate of Zn vapor is controlled and much less than that of heating Zn powders directly, although "the relatively high-saturated vapor pressure of Zn guarantees the concentration of this element necessary for the further growth of the Zn nanobelts".<sup>14</sup> However, all of the above have not been proven and further work should be done.

## Conclusion

In summary, by the simple method, that is, heating the raw materials without catalysts in a flowing gas at ambient pressure, Ga<sub>2</sub>O<sub>3</sub>, ZnO, and Si<sub>3</sub>N<sub>4</sub> nanowires, SiC nanowires, and SiO<sub>2</sub> amorphous nanowires have been obtained. The growth of these nanowires is dominated by the VS (or VLS) mechanism and the lower supersaturation may be a benefit to the growth of the nanowires other than particles. Because of the simplicity, low cost, and fewer number of necessary apparatuses, the present method thus has the advantage of manufacturing nanowires in bulk.

**Acknowledgment.** The authors thank Dr. Odile Stephan, Dr. Susana Trasobares, and Dr. Christian Colliex in the Laboratoire de Physique des solides, Université Paris-Sud, very much for their EELS spectra acquisition. The authors thank Prof. S. S. Fan for his help and discussion. This work is supported by the Nature Science Foundation of China, National 973 Project, 985 Project of Tsinghua University.

CM0201697

(15) Yang, P. D.; Lieber, C. M. *J. Mater. Res.* **1997**, *12*, 2981.

(16) Wu, Y. Y.; Messer, B.; Yang, P. D. *Adv. Mater.* **2001**, *13*, 1487.

(17) He, M. Q.; Minus, I.; Zhou, P. Z.; Mohammed, S. N.; Jacobs, R.; Sarney, W. L.; Salamanca-Riba, L.; Vispute, R. D. *Appl. Phys. Lett.* **2000**, *77*, 3731.

(18) Sears, G. W. *Acta Metall.* **1956**, *3*, 268.

(19) (a) Wang, M. J.; Wada, H. *J. Mater. Sci.* **1990**, *25*, 1690. (b) Jiang, G. J.; Zhuang, H. R.; Zhang, J.; Ruan, M. L.; Li, W. L.; Wu, F. Y.; Zhang, B. L. *J. Mater. Sci.* **2000**, *35*, 63. (c) Seo, W.; Koumoto, K. *J. Am. Ceram. Soc.* **1996**, *79*, 1777.

(20) Yumoto, H.; Hasiiguti, R. R. *J. Cryst. Growth* **1986**, *75*, 289.